HETEROCYCLES, Vol. 106, No. 2, 2023, pp. 277 - 289. © 2023 The Japan Institute of Heterocyclic Chemistry
Received, 24th October, 2022, Accepted, 5th December, 2022, Published online, 7th December, 2022
DOI: 10.3987/COM-22-14771

SUPRAMOLECULAR SELF-ASSEMBLY BASED ON SYMMETRIC TETRAMETHYL-SUBSTITUTED CUCURBIT[6]URIL AND SMALL AROMATIC AMINES

Lin Zhang, Jun Zheng, Xuanxun Wang, Zhu Tao, and Qianjun Zhang*

Key Laboratory of Macrocyclic and Supramolecular Chemistry of Guizhou Province, Institute of Applied Chemistry, Guizhou University, Guiyang 550025, China. *E-mail: Qianjun Zhang* - qjzhang@gzu.edu.cn

Abstract - In this paper, the interactions formed between symmetric tetramethyl-substituted cucurbit[6]uril (TMeQ[6]) and 4-cyanoaniline (CYA), 4,4'-methylenedianiline (MET), and 4-benzylaniline (BEN), were investigated using ^{1}H NMR spectroscopy and X-ray single crystal diffraction analysis. X-Ray single crystal diffraction showed that CYA was encapsulated in the cavity of TMeQ[6] and formed 1:1 host-guest complex **1**. Both MET and BEN were located at the TMeQ[6] portal and coordinated to form complex **2** and complex **3**, respectively, forming weak interactions with TMeQ[6], such as hydrogen bonding, C-H···π interactions, and ion-dipole interactions. Complexes **1**~**3** self-assemble to construct supramolecular nanoscale structures under the induction of $[ZnCl_4]^{2-}$ ions. The ^{1}H NMR spectroscopic analysis supported the crystallographic results in which an clathration or portal interaction occured between host and guest molecules.

INTRODUCTION

The cucurbit[n]urils (Q[n] or CB[n]) are another family of supramolecular organic compounds after crown ethers, cyclodextrins and calixarenes.[1-4] They are cyclic compounds formed by glycoluril units bridged by methylene groups, which contain a hydrophobic cavity and two hydrophilic portals.[5] At present, more than 100 cucurbit[n]urils have been reported,[6] among which ordinary cucurbit[n]urils include Q[5], Q[6], Q[7], etc.,[7,8] and a series of modified Q[*n*]s, such as methyl-,[9] cyclohexyl-,[10] cyclopentyl-,[11,12] hydroxyl-,[13] phenyl-[14] and cyclobutyl-cucurbit[*n*]uril[15] etc. The special structure and functional group properties of cucurbit[n]urils make them widely used in the field of host-guest chemistry, coordination chemistry and supramolecular self-assembly driven by non-covalent bonds including hydrogen bond, π···π conjugation, ion-dipole, dipole-dipole interactions.[16-22] Among them, supramolecular self-assemblies have the advantages of storage and multiphase catalysis due to their porous 1-D, 2-D and 3-D network structures, which have attracted significant interest toward using cucurbit[n]urils to synthesize nanolayers, pores and pipes. Various organic small molecules and ions are often used as components in supramolecular self-assembly frameworks.[23-33] For example, Feng et al.[34] constructed nine supramolecular self-assemblies consisting of Q[6], potassium salts, and phenol or its derivatives using traditional methods in 2010. In 2013, Ni et al.[35] reported that cucurbit[n]urils could interact with small aromatic molecules to form multidimensional supramolecular coordination structures and polymers under ion induction. Yan et al.[36] discovered that two aniline derivatives (benzidine and 4,4'-diaminodiphenylmethane) can coordinate with TMeQ[6] via the carbonyl oxygen on the portal as well as the methyl and methylene groups on the outer surface via hydrogen bond interactions and other non-covalent bonding interactions. Based on previous studies, we discussed three small aniline derivatives [4-cyanoaniline (CYA), 4,4'-methylenedianiline (MET) and 4-benzylaniline (BEN)] and studied their interactions with TMeQ[6] (Figure 1 and Scheme 1) using NMR spectroscopy and X-ray single crystal diffraction analysis, the purpose of this paper was to report the new supramolecular framework structures and provided available support for the subsequent research.

In this paper, ^{1}H NMR spectroscopy showed that all three aniline derivatives could interact with TMeQ[6]. CYA, MET and BEN interacted with TMeQ[6] by the inducer of $[ZnCl_4]^{2-}$ ions to form complexes **1**, **2** and **3**, respectively. The crystal structures of the complexes showed that CYA was located inside the cavity of TMeQ[6], whereas MET and BEN were located at the TMeQ[6] portal. The differences in their molecular size and substituents, the crystallographic parameters formed between the aniline derivatives and TMeQ[6] via non-covalent bond interactions were different (Table 1). Figure 2 shows the cell units of complex **1**,

complex **2**, and complex **3**, respectively. The number of molecules and ions in the cell unit were different, showing different interaction modes. At the same time, we obtained porous nanomaterials. These findings provided a theoretical basis for their applications.

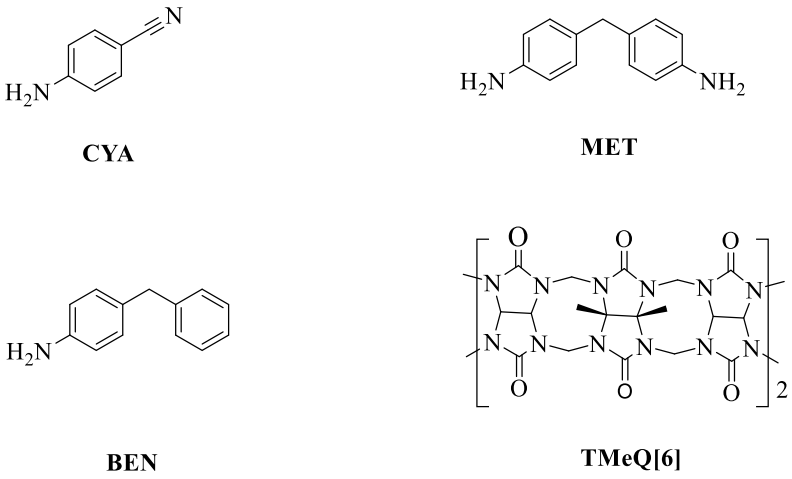

Figure 1. The molecular structure of CYA, MET, BEN and TMeQ[6]

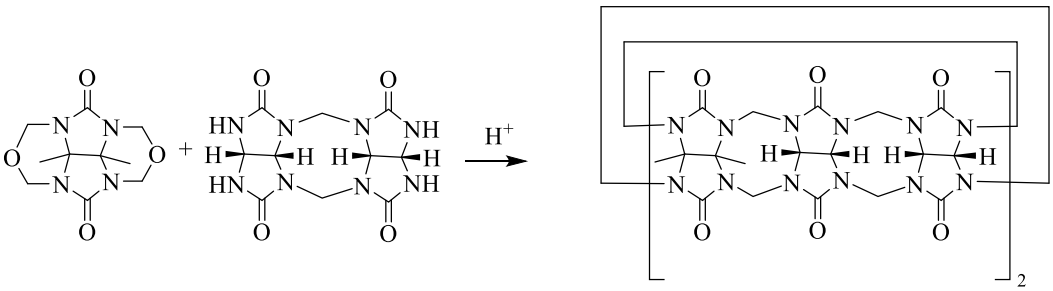

Scheme 1. Synthesis flow chart of TMeQ[6]

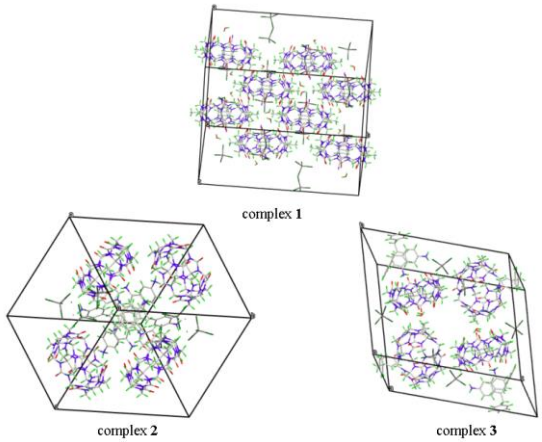

Figure 2. Crystal cell unit diagrams of complex **1**, complex **2** and complex **3**

RESULTS AND DISCUSSION

Crystal structure analysis of complexes 1~3:[37]

Transparent crystals without cracks were selected and tested with Bruker D8 VENTURE diffractometer and the crystals were analyzed，the crystal parameters and data acquisition conditions of CPE@Q[8] were measured (as shown in Table 1).

Table 1. Crystallographic Parameters of complex **1**, complex **2** and complex **3**

	Complex **1**	Complex **2**	Complex **3**
Empirical formula	$C_{47}H_{55}Cl_{7.5}N_{26}O_{14}Zn_2$	$C_{66}H_{76}Cl_8N_{28}O_{12}Zn_2$	$C_{119}H_{134}Cl_{12}N_{51}O_{26}Zn_3$
Formula weight	1604.78	1867.88	3316.27
Crystal system	monoclinic	triclinic	triclinic
Space group	C2/c	$P\bar{1}$	$P\bar{1}$
a[Å]	25.514(10)	16.196(4)	12.982(5)
b[Å]	33.507(10)	21.572(6)	25.563(10)
c[Å]	18.134(7)	24.111(7)	28.478(12)
α[°]	90	92.944(8)	112.834(12)
β[°]	114.809(14)	98.870(8)	90.524(12)
γ[°]	90	109.924(7)	93.767(13)
V[$Å^3$]	14072(9)	7776(4)	8685(6)
Z	8	3	2
D_{calcd}.[g cm^{-3}]	1.515	1.197	1.268
T[K]	273.15	273.15	273.15
μ[mm^{-1}]	1.043	0.729	0.668
Parameters	875	1586	1890
R_{int}	0.1062	0.1638	0.1008
R[I > 2σ(I)][a]	0.0724	0.1254	0.0824
wR[I > 2σ(I)][b]	0.2002	0.3368	0.2241
R(all data)	0.1396	0.2304	0.1496
wR(all data)	0.2303	0.3809	0.2487
GOF on F^2	1.004	1.073	1.020

[a] Conventional *R* on F*hkl*: $\sum||F_o| - |F_c||/\sum|F_o|$

[b] Weighted R on $|Fhkl|^2$: $\sum[w(F_o^2 - F_c^2)^2]/\sum[w(F_o^2)^2]^{1/2}$

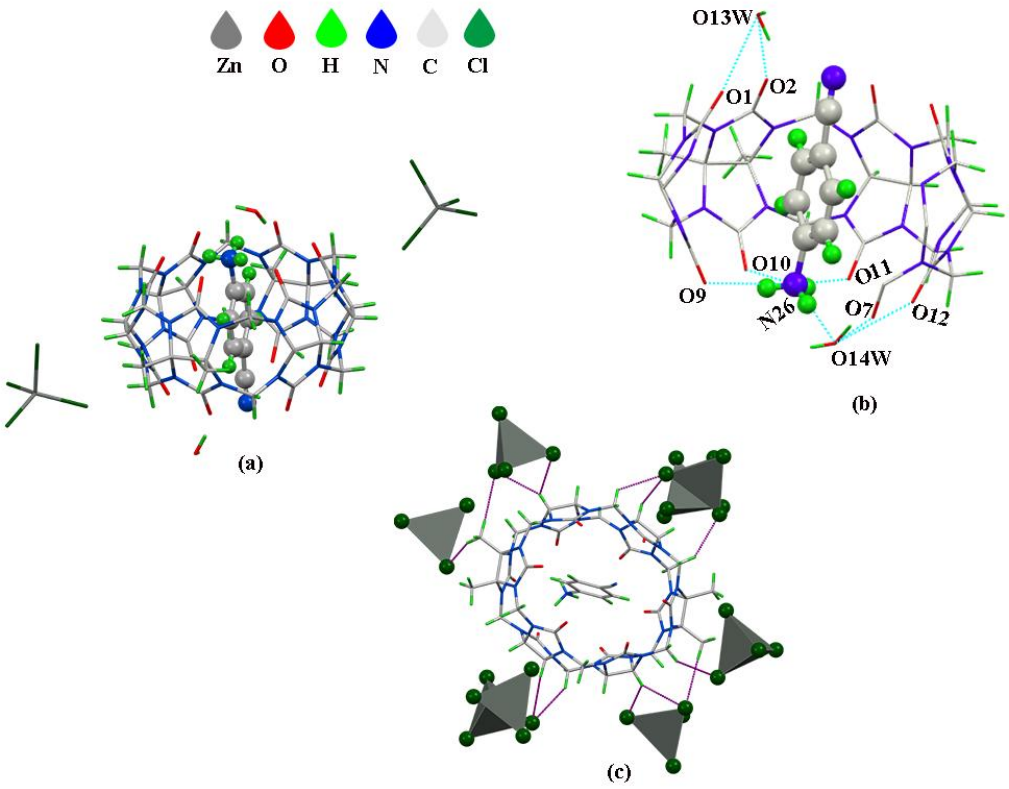

Figure 3. (a) The asymmetric unit of complex **1**, (b) hydrogen bond interactions, (c) ion-dipole

The crystal structure of complex **1** in Figure 3(a) showed that CYA interacted with TMeQ[6] to form 1:1 host-guest complex. Figure 3(b) shows that the two portals in TMeQ[6] interacted with a water molecule via hydrogen bond (O13W-O1, O13W-O2, O14W-O7 and O14W-O12). At the same time, CYA interacted with the portal carbonyl oxygen atoms in TMeQ[6] molecular via hydrogen bond, the interaction distances of N26-O9, N26-O10 and N26-O11 are 2.810Å, 3.036Å and 2.818Å, respectively. And O14W water molecule bridged the amino group of CYA with the carbonyl oxygen at the portal of TMeQ[6] via hydrogen bonds. In addition, each TMeQ[6] molecule bonded with eight $[ZnCl_4]^{2-}$ ions via ion-dipole interactions [purple curve in Figure 3(c)].

The asymmetric unit structure of the complex **2** crystal in Figure 4(a), contained three MET molecules, one point five TMeQ[6] molecules and three $[ZnCl_4]^{2-}$ ions. Figure 4(b) indicates that MET and TMeQ[6] was driven by a hydrogen bond interaction, and this distance is 2.716Å. Meanwhile, Figure 4(c) shows the amino groups of the another two MET molecules were directly bonded with the carbonyl oxygen atom of the TMeQ[6] portal via a hydrogen bond interaction, the range of interactions of N40-O18, N40-O15, N40-

O14, N38-O7, N38-O8, and N38-O9 is 1.915~2.817Å. A TMeQ[6] molecule was surrounded by four $[ZnCl_4]^{2-}$ ions via C-H···Cl, as shown in Figure 4(d).

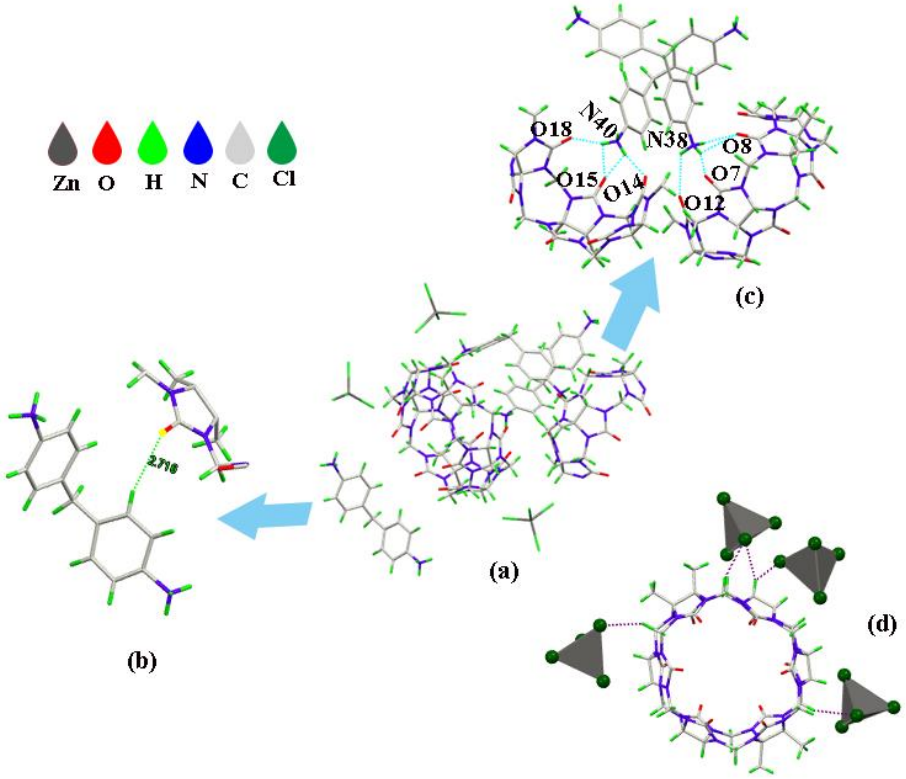

Figure 4. (a) The asymmetric unit of complex **2**, (b) weak interaction, (c) hydrogen bond interactions, (d) ion-dipole

From the asymmetric unit structure of complex **3** shown in Figure 5(a), it can be seen that when BEN interacted with TMeQ[6], BEN also interact with the portal of TMeQ[6], and there are ion-dipole interactions between $[ZnCl_4]^{2-}$ and TMeQ[6] or BEN molecules, as shown in the purple curve. Figures 5(b) and 5(c) show the interactions formed between BEN and TMeQ[6], in which the protonated amino group in BEN formed a hydrogen bond (N49-O19, N49-O20, N49-O21, N50-O23, N51-O11 and N51-O12) with the carbonyl oxygen at the portal of TMeQ[6]. Figure 5(d) shows the electrostatic interactions formed between the negative potential of the carbonyl oxygen at the portal of one TMeQ[6] and the positive potential on the outer surface of another TMeQ[6] (as shown in yellow curve), these interactions distances of C23-H···O18, C24-H···O18, C27-H···O13 and C31-H···O13 are 2.692, 2.363, 2.641, 2.687Å, respectively.

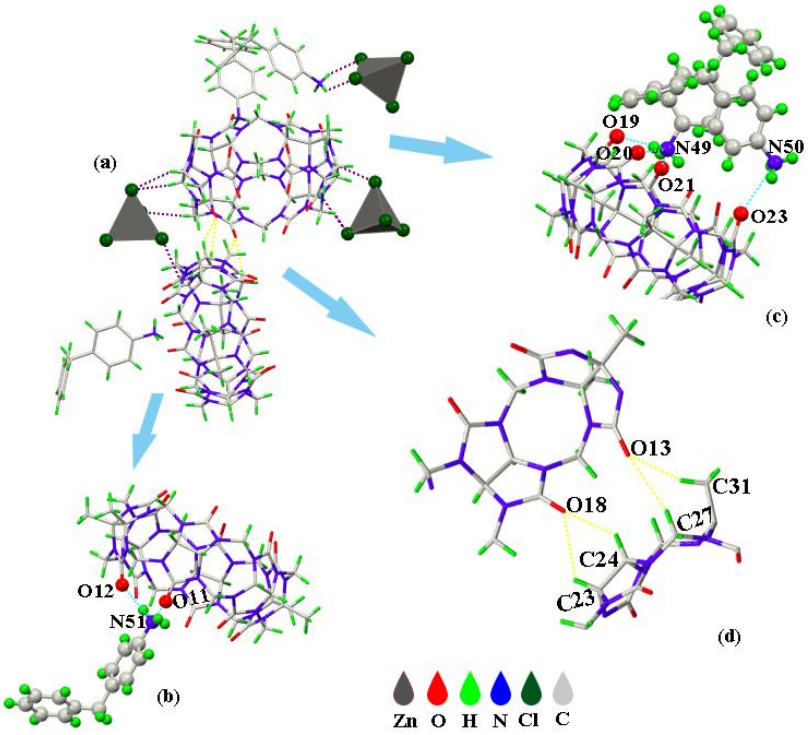

Figure 5. (a) The asymmetric unit of complex **3**, (b) and (c) hydrogen bond interactions, (d) is the dipole-dipole interaction between TMeQ[6]

The design and construction of supramolecular organic frameworks based on the interactions formed between organic molecules and ions is a hot research topic.[23-33] Figures 6(a)~8(a) show the accumulation of the complexes **1**~**3** along the *a*-axis, which clearly presented supramolecular frameworks are constructed under the bridging of $[ZnCl_4]^{2-}$ ions [Figures 6(b)~8(b)]. The structure of complex **2** is similar to layered stacking, and there are gaps between each layer; the structure of complex **3** is porous.

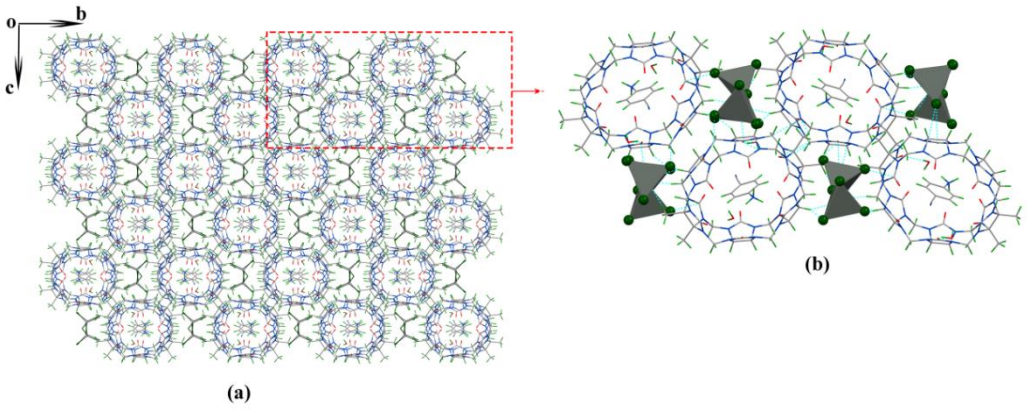

Figure 6. The accumulation structure of the complex **1** along the *a*-axis

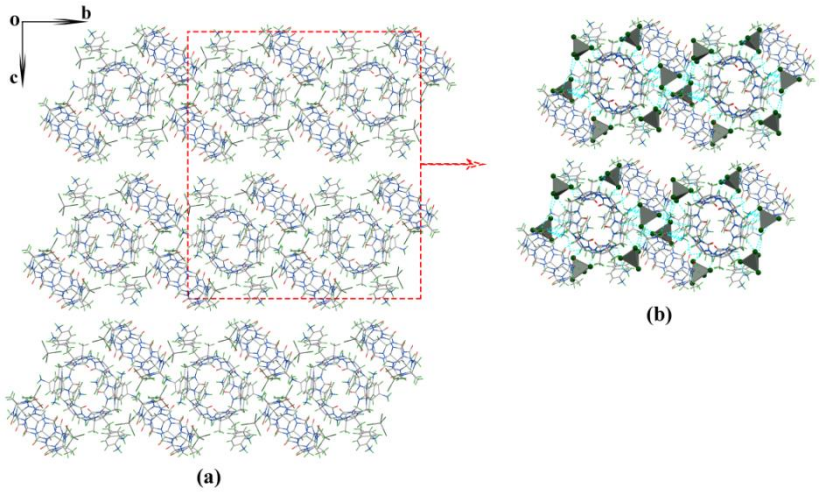

Figure 7. The accumulation structure of the complex **2** along the *a*-axis

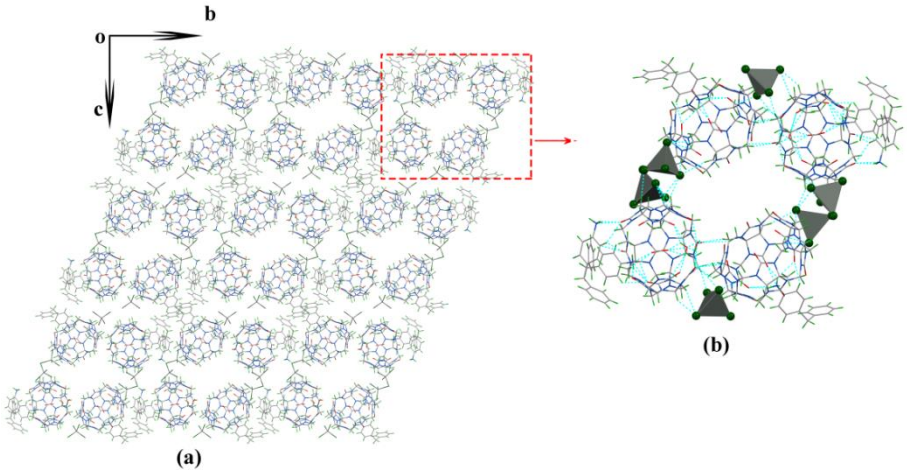

Figure 8. The accumulation structure of the complex **3** along the *a*-axis

^{1}H NMR spectroscopy analysis

^{1}H NMR spectroscopy is an important characterization method used to study host-guest interactions. When the guest molecule interacted with the inner part of the TMeQ[6], the proton peak of the guest molecule moved to the high field region, whereas when it interacted with the portal of the TMeQ[6], it moved to the low field region. In order to further clarify whether the coordination of TMeQ[6] and the three aniline derivatives in the solution were the same as the crystal state, we investigated the interactions formed between the three aniline derivatives and TMeQ[6] using ^{1}H NMR spectroscopy.

Table 2. Changes in the ^{1}H NMR chemical shifts of CYA after the addition of TMeQ[6]

^{1}H nucleus	1-H 4-H	2-H 3-H
$\Delta\delta$/ppm	-0.88	-0.79

*Δδ = δcomplex − δfree

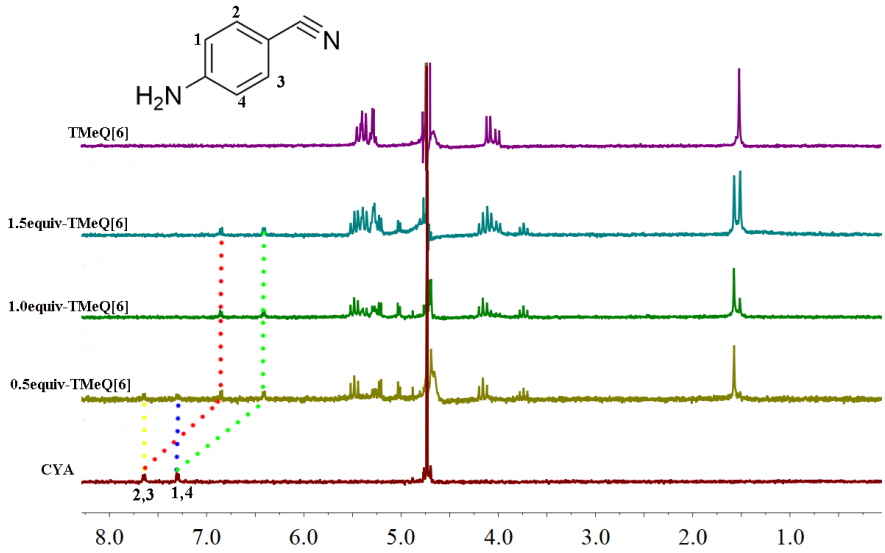

Figure 9. ^{1}H NMR titration spectra of CYA and TMeQ[6]

The results of the ^{1}H NMR titration study showed that when TMeQ[6] was added to the CYA , the proton peaks of TMeQ[6] were split; the H1, H2, H3 and H4 proton peaks of CYA moved significantly towards the high field region. When n(TMeQ[6]):n(CYA) = 1:1, all of the proton characteristic peaks were located in the high field region, as shown in Figure 9 and Table 2. Therefore, all of the CYA molecules entered the cavity of TMeQ[6] and formed 1:1 host-guest complex. In addition, the ^{1}H NMR spectra of the interaction between MET and BEN with TMeQ[6] showed the proton peaks of MET or BEN moved towards the low field region, chemical shift was shown in Tables 3 and 4, both interact with the portal of TMeQ[6] (Figures 10 and 11).

Table 3. Changes in the ^{1}H NMR chemical shifts of MET after the addition of TMeQ[6]

^{1}H nucleus	1,2,3,4,5,6,7,8,9-H	5-H
$\Delta\delta$/ppm	0.04	0.02

*Δδ = δcomplex − δfree

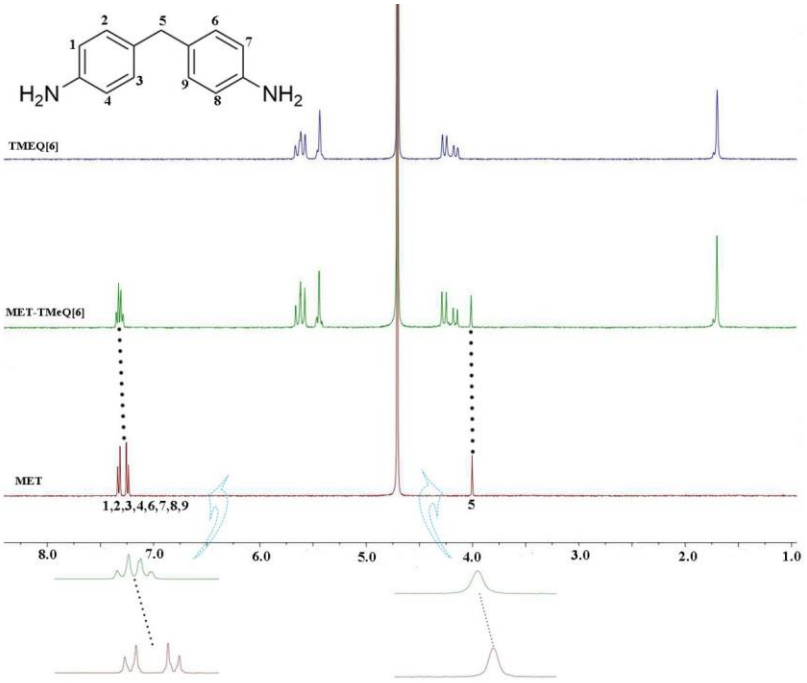

Figure 10. ^{1}H NMR titration spectra of MET and TMeQ[6]

Table 4. Changes in the ^{1}H NMR chemical shifts of BEN after the addition of TMeQ[6]

^{1}H nucleus	1,2,3,4,5,6,7,8,9,10-H	5-H
$\Delta\delta$/ppm	0.02	0.02

$^{*}\Delta\delta = \delta\text{complex} - \delta\text{free}$

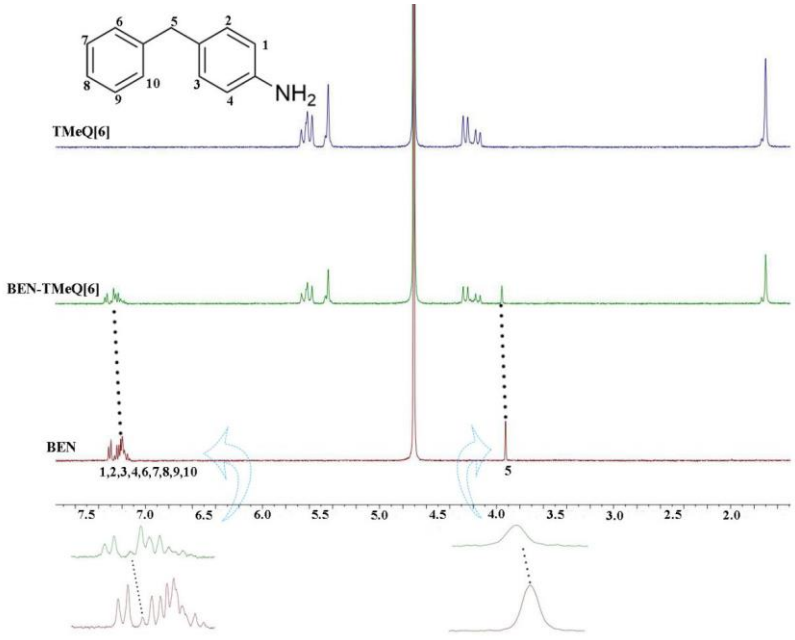

Figure 11. ^{1}H NMR titration spectra of BEN and TMeQ[6]

CONCLUSION

In summary, the interactions formed between TMeQ[6] and CYA, MET, and BEN have been investigated using ^{1}H NMR spectroscopy. The results showed that MET and BEN were located at the portal of TMeQ[6] and CYA entered the TMeQ[6] cavity to form 1:1 host-guest complex **1**. And X-ray single crystal diffraction analysis complexes **1**~**3** constructed supramolecular framework structure under the induction of $[ZnCl_4]^{2-}$ ions.

EXPERIMENTAL

Reagent: All materials were reagent grade and used without any further purification. TMeQ[6][38] (purity ≥97%) was prepared in the Key Laboratory of Macrocyclic and Supramolecular Chemistry of Guizhou Province, China, and the synthetic route is shown in Scheme 1. CYA, MET and BEN were all purchased from Shanghai Titan Scientific Co., Ltd with a purity of 98%.

Apparatus: Bruker D8 VENTURE diffractometer; JNM-ECZ400s MHz Nuclear Magnetic Resonance System (JEOL); AKHL-III-08 Eco laboratory ultrapure water machine (Chengdu Eco Water Treatment Equipment Co., Ltd.; an instrument for preparing deionized water); FA2204N Electronic Balance (Shanghai Jinghai Instrument Co., ltd).

Experiments for Crystal Growing: When growing crystals, we often use $ZnCl_2$ or $CdCl_2$ as structural inducers, which helps to grow crystals and enhance the symmetry of crystal structure. Here, we take a small amount of $ZnCl_2$ as the inducer, Weigh 0.005 g CYA and 0.045 g TMeQ[6], 0.005 g MET and 0.026 g TMeQ[6], 0.005 g BEN and 0.029 g TMeQ[6], respectively, add 1.5 mL (0.1 mol/L) formic acid aqueous solution to dissolve by heating, after placeing for a period of time at room temperature, the solvent was evaporated to precipitate massive transparent crystals (the yield thereof was 35%), three complexs are measured. The complexs formed by TMeQ[6] and CYA, MET or BEN are uniformly named as complex **1**, complex **2** and complex **3**, respectively.

Instrument Characterization Methods and Test Conditions: Crystals without transparency and crack at room temperature are selected, and the data of complexes **1**~**3** are collected by using a Bruker D8 Venture X-ray single crystal diffraction X-ray in Scan mode using a graphite monochro-matic Mo-K ray (λ= 0.71073 Å, μ = 0.828 mm^{-1}) in ω-scan mode. Lorentz polarization and absorption corrections were applied. Structural solutions and full-matrix least-squares refinements based on F2 were performed using the SHELXT-14 and SHELXL-14 program packages, respectively. Analytical expressions of the neutral-atom

scattering factors were employed and anomalous dispersion corrections were incorporated. All nonhydrogen atoms were refined anisotropically. Most of the water molecules in the compounds were omitted using the SQUEEZE option in the PLATON program. The main crystal structure parameters are shown in Table 1.

Determination of the ^{1}H NMR Spectroscopy: ^{1}H NMR spectra of the interaction between TMeQ[6] and CYA, MET or BEN in 0.1M DCl environment were recorded at 20 ºC on a JNM-ECZ400s MHz nuclear magnetic resonance spectrometer.

ACKNOWLEDGEMENTS

The Science and Technology Support Plan of Guizhou Province [GuiZhouScience and Technology Cooperation Support (2020) 4Y218] is acknowledged.

REFERENCES AND NOTES

1. N. Saleh, A. L. Koner, and W. M. Nau, *Angew. Chem. Int. Ed.*, 2008, **47**, 5398.
2. X. J. Cheng, L. L. Liang, K. Chen, N. N. Ji, X. Xiao, J. X. Zhang, Y. Q. Zhang, S. F. Xue, Q. J. Zhu, X. L. Ni, and Z. Tao, *Angew. Chem. Int. Ed.*, 2013, **52**, 7252.
3. Q. Li, S. C. Qiu, J. Zhang, K. Chen, Y. Huang, X. Xiao, Y. J. Zhang, F. Li, Y. Q. Zhang, S. F. Xue, Q. J. Zhu, Z. Tao, L. F. Lindoy, and G. Wei, *Org. Lett.*, 2016, **18**, 4020.
4. A. I. Day, R. J. Blanch, A. P. Amold, S. Lorengo, G. R. Lewis, and I. Dance, *Angew. Chem. Int. Ed.*, 2002, **41**, 275.
5. Z. S. Zeng, J. Xie, G. Y. Luo, Z. Tao, and Q. J. Zhang, *Beilstein J. Org. Chem.*, 2020, **16**, 2332.
6. C. Liu, R. H. Gao, Y. Q. Zhang, Q. J. Zhu, and Z. Tao, *Chinese Chem. Lett.*, 2021, **32** 362.
7. W. A. Freeman, W. L. Mock, and N. Y. Shih, *J. Am. Chem. Soc.*, 1981, **103**, 7367.
8. J. Kim, I. S. Jung, S. Y. Kim, E. Lee, J. K. Kang, S. Sakamoto, K. Yamaguchi, and K. Kim, *J. Am. Chem. Soc.*, 2000, **122**, 540.
9. Y. Meng, W. W. Zhao, J. Zheng, D. F. Jiang, J. Gao, Y. M. Jin, and P. H. Ma, *RSC Adv.*, 2021, **11**, 3470.
10. J. Zhao, H. J. Kim, J. Oh, S. Y. Kim, J. W. Lee, S. Sakamoto, K. Yamaguchi, and K. Kim, *Angew. Chem.*, 2001, **113**, 4363.
11. F. Wu, L. H. Wu, X. Xiao, Y. Q. Zhang, S. F. Xue, Z. Tao, and A. I. Day, *J. Org. Chem.*, 2012, **77**, 606.
12. L. H. Wu, X. L. Ni, F. Wu, Y. Q. Zhang, Q. J. Zhu, S. F Xue, and Z. Tao, *J. Mol. Struct.*, 2009, **920**, 183.
13. S. Y. Jon, N. Selvapalam, D. H. Oh, J. K. Kang, and K. Kim, *J. Am. Chem. Soc.*, 2003, **125**, 10186.

14. H. Isobe, S. Sato, and E. Nakamura, *Org. Lett.*, 2002, **4**, 1287.
15. M. H. Chen, N. X. Lv, W. W. Zhao, and A. I. Day, *Molecules*, 2021, **26**, 7343.
16. J. Lagona, P. Mukhopadhyay, S. Chakrabarti, and L. Isaacs, *Angew. Chem. Int. Ed.*, 2005, **44**, 4844.
17. J. W. Lee, S. Samal, N. Selvapalam, H. J. Kim, and K. Kim, *Acc. Chem. Res.*, 2003, **36**, 621.
18. O. A. Gerasko, D. G. Samsonenko, and V. P. Fedin, *Russ. Chem. Rev.*, 2002, **71**, 741.
19. J. Elemans, A. E. Rowan, and R. Nolte, *Ind. Eng. Chem. Res.*, 2000, **39**, 3419.
20. T. J. Hubin, A. G. Kolchinski, A. L. Vance, and D. H. Busch, "*Template Control of Supramolecular Architecture*", *Advances in Supramolecular-Chemistry*, 1999, **5**, 237.
21. W. L. Mock, *Top. Curr. Chem.*, 1995, **175**, 1.
22. P. Cintas, *J. Inclusion Phenom. Mol. Recognit. Chem.*, 1994, **17**, 205.
23. M. Fujita, Y. J. Kwon, S. Washizu, and K. Ogura, *J. Am. Chem. Soc.*, 1994, **116**, 1151.
24. R. E. Norman, N. J. Rose, and R. E. Stenkamp, *J. Chem. Soc., Dalton Trans.*, 1987, **1**, 2905.
25. S. Subramanian and M. J. Zaworotko, *Angew. Chem., Int. Ed. Engl.*, 1995, **34**, 2127.
26. D. Bradshaw, T. J. Prior, E. J. Cussen, J. B. Claridge, and M. J. Rosseinsky, *J. Am. Chem. Soc.*, 2004, **126**, 6106.
27. H. Li, C. E. Davis, T. L. Groy, D. G. Kelley, and O. M. Yaghi, *J. Am. Chem. Soc.*, 1998, **120**, 2186.
28. S. Q. Ma, J. Eckert, P. M. Forster, J. W. Yoon, Y. K. Hwang, J. S. Chang, C. D. Collier, J. B. Parise, and H. C. Zhou, *J. Am. Chem. Soc.*, 2008, **130**, 5896.
29. O. Ohmori and M. Fujita, *Chem. Commun.*, 2004, 1586.
30. J. S. Seo, D. Whang, H. Lee, S. I. Jun, J. Oh, Y. J. Jeon, and K. Kim, *Nature*, 2000, **404**, 982.
31. M. E. Davis, *Nature*, 2002, **417**, 813.
32. A. Corma, *J. Catal.*, 2003, **216**, 298.
33. G. Ferey, *Science*, 2001, **291**, 994.
34. X. Feng, H. Du, K. Chen, X. Xiao, S. X. Luo, S. F. Xue, Y. Q. Zhang, Q. J. Zhu, Z. Tao, X. Y. Zhang, and G. Wei, *Cryst. Growth Des.*, 2010, **10**, 2901.
35. X. L. Ni, X. Xiao, H. Cong, L. L. Liang, K. Chen, X. J. Cheng, N. N. Ji, Q. J. Zhu, S. F. Xue, and Z. Tao, *Chem. Soc. Rev.*, 2013, **42**, 9480.
36. Y. Yan, S. F. Xue, H. Cong, J. X. Zhang, Y. Q. Zhang, Q. J. Zhu, and Z. Tao, *New J. Chem.*, 2009, **33**, 2136.
37. All parameters of this crystal are stored in the Cambridge Crystallographic Data Centre, the publication numbers of the three complexes, complex **1**, complex **2** and complex **3**, are 2163797, 2153558, 2167469, respectively.
38. Y. J. Zhao, S. F. Xue, Q. J. Zhu, Z. Tao, J. X. Zhang, Z. B. Wei, L. S. Long, M. L. Hu, H. P. Xiao, and A. I. Day, *Chin. Sci. Bull.*, 2004, **49**, 1111.